TÜBİTAK

Turkish Journal of Earth Sciences

http://journals.tubitak.gov.tr/earth/

Research Article

Turkish J Earth Sci
(2023) 32: 685-702
© TÜBİTAK
doi:10.55730/1300-0985.1868

Spherical Bouguer effect of topography on gravity with constant and laterally varying density

Mehmet SİMAV
General Directorate of Mapping, Tıp Fakültesi Caddesi, Ankara, Turkey

Received: 15.12.2022 • **Accepted/Published Online:** 08.06.2023 • **Final Version:** 28.07.2023

Abstract: Gravitational attraction of the Earth's visible topography above the mean sea level is generally regarded as an unwanted signal in various geoscience applications. It should be removed from the observations to reveal the remaining signals of subsurface anomalous density distribution or to satisfy the boundary condition in solving the geodetic boundary value problems. However, the task of determining the gravimetric terrain effects involves tedious numerical computations when high-resolution elevation data is used. While the traditional computational approach relies on flat-Earth approximation and neglects the topographic masses beyond some fixed integration radius, e.g., planar complete Bouguer correction, the modern methods apply spherical-Earth approximation and consider the far zone contribution, e.g., spherical complete Bouguer correction. This study compares the planar and spherical complete Bouguer corrections with constant topo-density at two test areas in Turkey, then assesses the performance of the recently released ultra-high resolution SRTM2gravity model in the same regions. Moreover, the first lateral global topographical density model (UNB_TopoDens) has been employed to quantify the effect of topographic mass-density anomalies on gravity across the study areas. The numerical investigations have shown that simple planar complete Bouguer corrections exhibit similar spatial structure to those of the spherical counterparts, but with different magnitudes. There exists an average bias of around 30 mGal between the planar and spherical Bouguer correction because the latter takes the gravitational attraction of global topography into account. The SRTM2gravity model performs exceptionally well in the test regions and can directly be used to derive spherical Bouguer corrections over land areas with little computational effort. The topo-density anomalies may induce gravity effects up to 60 mGal, particularly over the mountainous parts of the study regions. This considerable amount of contribution should be treated carefully and cautiously especially in geodetic applications since the solution of geodetic boundary problems requires rigorous compensation of topographical gravity effects with actual density distribution. The results of the study are also hoped to give insights into the reproduction of the forthcoming regional Bouguer anomaly map of Turkey.

Key words: Forward gravity field modelling, spherical Bouguer correction, planar Bouguer correction, SRTM2gravity model, UNB_TopoDens model, topographic mass-density anomaly

1. Introduction

It is a common procedure to use a frequency division model in the Earth's gravity field modelling, i.e. the separation of long, middle, and short-wavelength signals each of which is generated by different sources. Some of them may be regarded as extraneous effects which need to be properly treated as reductions or corrections to isolate the target sources. The topographic masses above the mean sea level account for the high-frequency variations and their associated gravity effects are generally removed from the gravity field observations in many practical applications of the gravimetry, i.e. complete or refined Bouguer correction. The applications include the gravity data inversion, interpretation, and solution of geodetic boundary value problem where the topography is not the focus of the study (Heiskanen and Moritz, 1967; Hinze et al., 2013).

The negative vertical or radial derivative of the gravitational potential of global topographic masses at a computation point on or above the Earth's surface is denoted as the gravitational attraction of topography. Reduction of the actual gravity from the attraction of topographic masses is designated as topographic mass reduction or complete Bouguer reduction (Forsberg, 1984; Li and Sideris, 1994; Featherstone and Kirby, 2002; Vajda et al., 2020). The gravity effect of global topographic masses A^t located at a point P with a given spherical latitude φ_P, spherical longitude λ_P, and height H_P above the mean sea level can be calculated through the evaluation of Newton's

* Correspondence: mehmet.simav@harita.gov.tr

volume integral in spherical coordinates as follows (Vajda et al., 2004):

$$A^t(r_P,\varphi_P,\lambda_P) = -G\int_{\varphi'=-\pi/2}^{\pi/2}\int_{\lambda'=0}^{2\pi}\int_{r'=R}^{R+H'}\rho^t(\varphi',\lambda',r')\frac{\partial L^{-1}(r_P,\psi,r')}{\partial r_P}r'^2\cos\varphi' d\varphi' d\lambda' dr' \quad (1)$$

where R is the radius of the geocentric sphere and r_P is the geocentric radius of the computation point P, e.g., $r_P = R + H_P$. The term G is Newton's gravitational constant and $\rho^t(\varphi',\lambda',r')$ is the topographic density at the integration points usually assumed to be constant $\rho^t = 2670\ \mathrm{kgm^{-3}}$. The $\partial L^{-1}(r_P,\psi,r')/\partial r_P$ term in Eq. (1) represents the radial derivative of the reciprocal spatial distance. The spatial distance L between the computation and running points can easily be computed using the spherical coordinates based on the law of cosines in plane and sphere geometry as follows:

$$L = L(r_P,\psi,r') = \sqrt{r_P^2 + r'^2 - 2r_P r'\cos\psi} \quad (2)$$

$$\cos\psi = \cos\varphi_P\cos\varphi' + \sin\varphi_P\sin\varphi'\cos(\lambda_P - \lambda') \quad (3)$$

While the basic formulas for the calculation of the gravimetric terrain effect may look relatively straightforward, the precise evaluation is one of the most time-consuming and labor-intensive processes in gravity field modelling due to the irregular structure of the topographic surfaces bounding the masses. The volume integral in Eq. (1) should extend over the whole globe in principle, and today we have very high-resolution global digital elevation and density models which together end up tedious and tremendous numerical computations.

Many procedures for an efficient calculation of the topographic effect on gravity in space and frequency domains have been proposed so far. The traditional approach relies on approximations such as planarization and neglecting the topographic masses beyond some fixed integration radius to reduce the computation time. The attraction of topographic masses is split into two parts: the attraction of a Bouguer plate of constant density and the attraction of the residual terrain which is also usually denoted as terrain correction (Heiskanen and Moritz, 1967). The major part of the topographic reduction is attributed to an infinite Bouguer plate, i.e. the A^B term on the right side of Eq. (4), which can easily be calculated by simple multiplication. Under a linear and planar approximation, the classical terrain correction formula, i.e. the A^{TC} term on the right side of Eq. (4), is given as follows (Moritz, 1968; Li and Sideris, 1994; McCubbine et al., 2017):

$$A^t(x_P,y_P,\mathrm{H}_P) = A^B - A^{TC} = 2\pi G\rho^t H_P - \frac{G\rho^t}{2}\iint_\sigma \frac{(H'-H_P)^2}{l^3}dx'dy' \quad (4)$$

$$l = \sqrt{(x'-x_P)^2 + (y'-y_P)^2} \quad (5)$$

where x and y denote the plane coordinates. The term l is the planar distance between computation and running points. The surface area σ that the integral in Eq. (4) is evaluated is such that $(x',y') \in \sigma$ if $< l < S$, where S is the integration radius (e.g., 167 km) beyond which the contribution to the terrain correction is negligible. To the best of the author's knowledge, the official Bouguer anomaly map of Turkey has been computed by the traditional approach (Arslan, 2016).

The contemporary complete Bouguer correction computations, however, are based on more accurate spherical approximation incorporating the whole topographic masses around the globe (see Eq. (1)), because the classical approach approximates the shape of the topography very poorly. Hirt et al. (2019) have computed an ultra-high resolution model of spherical complete Bouguer corrections with nearly global coverage recently. They have converted 3" (~90 m) resolution Shuttle Radar Topography Mission (SRTM) digital elevation data to implied spherical topographic gravity effects and produced *SRTM2gravity* modern correction model. The model covers the Earth's land areas within 60°S to 85°N geographic latitude and comprises ~28 billion computation points. This exceptional model has some limitations such that it disregards the mass-density anomalies and relies solely on the constant mass-density assumption (e.g., 2670 $\mathrm{kgm^{-3}}$) and its approximation errors are expected to be largest over the narrow and deep mountain valleys.

Sheng et al. (2019) have recently developed the first laterally varying global topographical density model and released it under the name *UNB_TopoDens*. The model spans the globe at 30" (~900 m) resolution and has already been validated against present-day global and regional topographical density models. Results suggest the model provides a satisfactory agreement and recommend using it for investigations of the crust and mantle, isostasy, and gravimetric studies.

With these issues in mind, the first goal of this study is to quantify and compare the traditional planar and modern spherical methods of complete Bouguer computations in two test areas in Turkey covering the roughest part of the country where the topographic and gravity field variations are highly complex and where the forward modelling errors can be expected to be the largest. The next analysis assesses the performance of the SRTM2gravity global and

spherical gravimetric complete Bouguer correction model in the same test regions. The last objective of the study is to quantify the contribution of the 2D UNB_TopoDens global topographical density model to reveal the effect of topographic mass-density anomalies on gravity relative to the reference density of 2670 kgm^{-3}. Section 2 describes the methodology for forward modelling of the gravimetric topographical effects. The third part explains the test regions and data used in the study. Section 4 presents and evaluates the results. The summary and conclusions are given in the last section.

2. Methodology

The Newtonian volume integral in Eq. (1) can be evaluated in the space domain based on mass discretization into elementary geometrical bodies such as polyhedra, inclined-top prisms, rectangular prisms, tesseroids, point masses, mass lines, mass layers, and/or concentric circles (Hammer, 1939; Nagy et al., 2000; Heck and Seitz, 2007; Wild-Pfeiffer, 2008; Kuhn et al., 2009; Tsoulis, 2012; Grombein et al., 2013; D'Urso, 2013; Uieda et al., 2016; Yang et al., 2020), then the superposition principle is applied to sum up the effects of all individual mass bodies. The triple integral can also be evaluated numerically using some quadrature methods (Asgharzadeh et al., 2007). Alternatively, the integration over the radial coordinate in the respective volume integral can be performed analytically, i.e. $\int_{r'=R}^{R+H_P} \frac{\partial L^{-1}(r_P,\psi,r')}{\partial r_P} r'^2 dr'$, then 2D surface integral can be evaluated numerically (Martinec, 1998; Novák, 2000; Novák et al. 2001). The Newton's integral in Eq. (1) has been evaluated through a global 2D numerical integration in the spatial domain with constant and laterally varying topographic density to obtain reference values for further comparisons. The in-house software developed by the author (Simav and Yıldız, 2021) has been used for the computations.

It is acknowledged that the computation time is directly related and linearly increases with the number of computation points and the number of mass elements of the digital elevation model (DEM), i.e. the more the number of computation points and/or higher the resolution of DEM the longer the computation time. It is also a well-known fact that the gravity effect of the topographic masses decreases with increasing distance from the computation point. Therefore, the integration domain is generally split into two zones in practice, a finer resolution DEM grid for the near zone and a coarser grid for the far zone are used to reduce computational costs. Cascading grid resolutions have been utilized with 3" in the near zone which extends up to a spherical distance of 1.5° from any computation point, and 15' DEM data for the far zone (the remainder to the full globe) effects.

The traditional planar gravimetric terrain computations have been performed by evaluating the Eqs. (4) and (5). The convolution integral of classical terrain correction, i.e. the A^{TC} term in Eq. (4) has been numerically integrated using rectangular prisms with the computation point coinciding with the origin of the coordinate system (Nagy, 1966; Nagy et al., 2000) utilizing again the in-house software developed by the author. The integration radius has been extended to a spherical distance of 1.5° (~167 km) and 3" high-resolution DEM data has given input to the software. It should be noted that the in-house software takes the Earth's curvature into account through the use of super elevation formulation given in Forsberg (1984). The terrain correction integral has also been implemented in the frequency domain by means of 2D direct and inverse fast Fourier transforms (2D FFT) (Forsberg, 1985; Sideris, 1985; Li and Sideris, 1994; McCubbine et al., 2017) and compared to the spatial domain method in both study regions. Although the mean of the differences between the two techniques is close to zero with a standard deviation of a few mGals, the extremes can reach up to 60 mGal in both study areas, particularly over the rugged terrains. Although the 2D FFT is extremely faster than the rectangular prisms, it is not recommended to apply in areas with high topographic gradients exceeding 45° (Martinec et al.,1996; Tsoulis, 2001). Therefore, spatial domain results are used for further analysis.

The values of Newton's gravitational constant, the radius of the geocentric sphere, and the constant topographic density are chosen similar to those adopted in the production of the SRTM2gravity model (Hirt et al., 2019), such that G= 6.67384 × 10^{-11} m^{3}kg^{-1}s^{-2}, R= 6378137.0 m, and p^t=2670 kgm^{-3}, respectively.

3. Study area & data description

Numerical analyses have been performed in two 1° × 1° quadrangle areas, the first one is on the southwestern coast of Turkey bounded by 36°N–37°N and 29°E–30°E (hereinafter referred to as N36E029), the second is in the northeastern coast of Turkey bounded by 40°N–41°N and 40°E–41°E (hereinafter referred to as N40E040). The study areas are located in regions that embody both land and sea parts containing diverse topography of hills, mountains, and low-lying deltas as well as relatively deep-sea trenches where the topographic and gravity field variations are highly complex. While the elevation ranges from 0 m to 3053 m with a standard deviation of 577 m within the surroundings of the first test area, the second is a bit higher with a maximum elevation of 3895 m. Figure 1 shows the boundaries and surrounding topography of the study regions. Computations have been done at 1' × 1' equiangular grid on the Earth's surface which comprises 3600 computation points in each region. The heights of the onshore computation points have

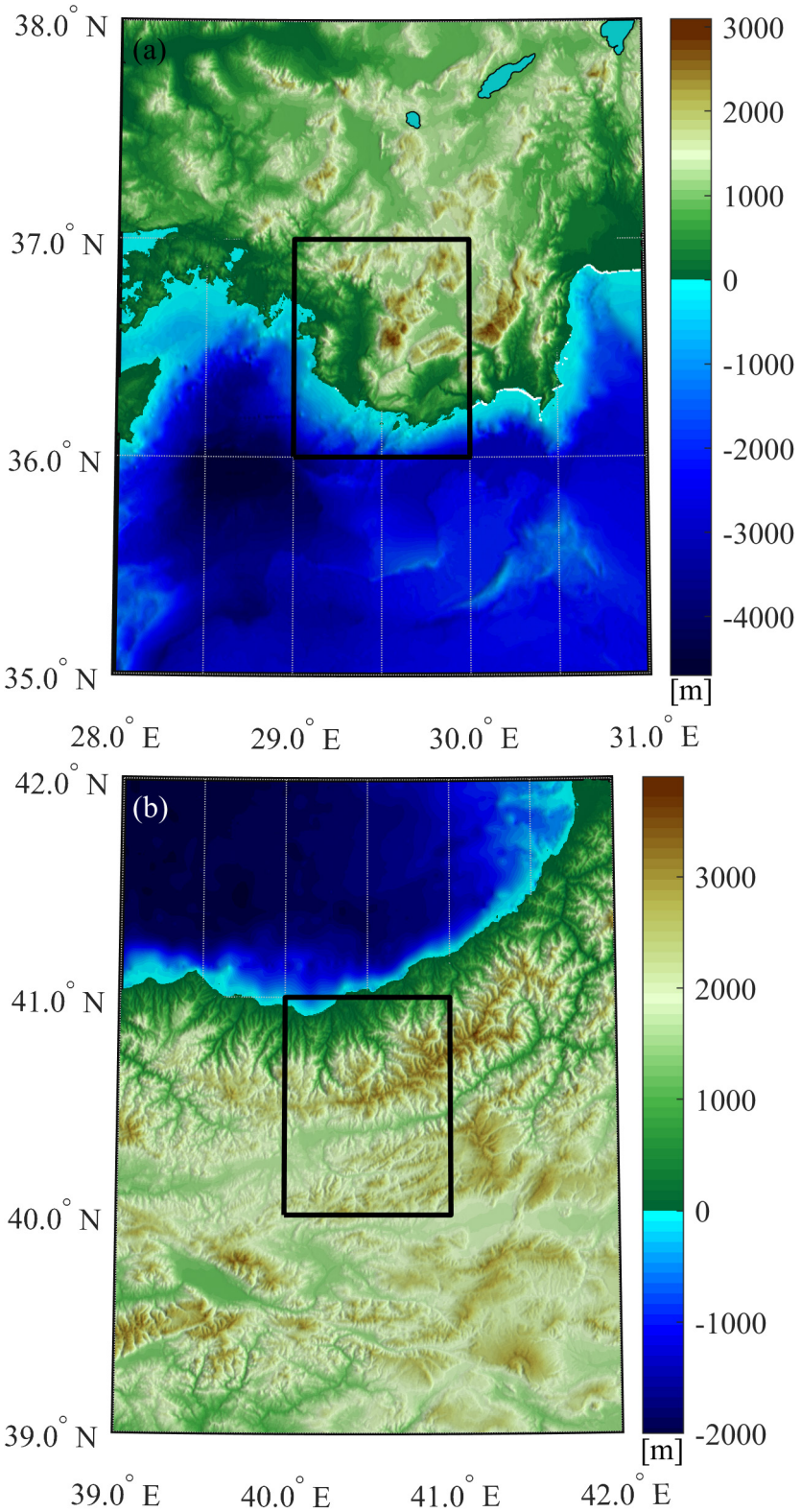

Figure 1. Location and topography of the 1° × 1° wide study areas (black rectangles) which cover two SRTM2gravity model tiles. (a) N36E029 in the southwestern coast of Turkey bounded by 36°N–37°N and 29°E–30°E, (b) N40E040 in the northeastern coast of Turkey bounded by 40°N–41°N and 40°E–41°E.

been determined from a high-resolution DEM and offshore point elevations are set to zero (e.g., on the sea surface).

Two different freely available terrain data are used for the evaluation of the terrain gravity effects. The first one is the high-resolution DEM from the Multi-Error-Removed Improved-Terrain DEM (MERIT DEM) project (Yamazaki et al., 2017). It is also the key input data set to the SRTM2gravity model (Hirt et al., 2019). The MERIT DEM model has a spatial resolution of 3" without bathymetry information and can be accessed from the developer's webpage at http://hydro.iis.u-tokyo.ac.jp/~yamadai/MERIT_DEM/. As already described in the previous section, this high-resolution model has been employed (i) to determine the heights of computation points on land, e.g., H_P, (ii) to compute spherical topographic effects within the near zone, and (iii) to calculate the classical planar terrain correction term.

The second SRTM data set used in the study is the SRTM15+ global bathymetry and topography model which is an updated version of the SRTM+ series (Becker et al., 2009; Olson et al., 2016). The MERIT DEM model has no global coverage and is limited to ±60° latitudes. On the other hand, SRTM15+ (Tozer et al., 2019) covers the whole globe with a spatial resolution of 15". The original SRTM15+ data is resampled to 15' by box averaging method and then the resulting data is employed to compute spherical topographic effects within the far zone. The SRTM15+ is publicly available and can be accessed from https://topex.ucsd.edu/WWW_html/srtm15_plus.html.

One of the objectives of this study is to assess the performance of the SRTM2gravity model in the study areas as already mentioned in the introduction. Briefly, the SRTM2gravity is an ultra-high resolution model of spherical complete Bouguer correction with nearly global coverage. It has been computed by combining spatial and spectral gravity forward modelling techniques with advanced computational resources in parallel. More information about the computational strategy can be found at Hirt et al. (2019). The model is provided at 1° tiles and is freely available via https://ddfe.curtin.edu.au/models/SRTM-2gravity2018/. The 3" spatial resolution N36E029 and N40E040 binary tiles each containing 1200 × 1200 values in cell-centered registration have been used for the analysis (see Figure 2). While the minimum values (i.e. less than 30 mGal) within the study areas are observed over the low-lying coastal areas and offshores, the corrections over the hills and mountains exceed 200 mGal with extreme values up to 317 mGal in the southwestern region and 387 mGal in the northeastern region. The high-resolution SRTM-2gravity data values are linearly interpolated at the computation points distributed with a constant spacing of 1' across the study regions.

The first laterally varying global topographical density model namely UNB_TopoDens has been used for the completion of the final study objective. The model is computed through the application of a high-resolution lithological map, i.e. the Global Lithology Model (GLiM) (Sheng et al., 2019). Assigning probable surface density values and error estimates to the lithologies based on geological data, the GLiM is transformed into UNB_TopoDens. The model is provided at three different grid spacings at https://gge.ext.unb.ca/Resources/TopographicalDensity/. The associated data files are in a native binary file structure utilized by the Generic Mapping Tools (GMT) software (Wessel et al., 2019). The GMT commands can be used to transform the data files into other formats. The 30s_UNB_TopoDens_2v01 data file has been used in this study. The anomalous topographic mass densities relative to the reference density of 2670 kgm$^{-3,}$ have been calculated, e.g., $\Delta\rho^t(\varphi', \lambda') = \rho^t(\varphi', \lambda') - 2670$, and the resulting mass-density anomalies are linearly interpolated at 3" MERIT DEM and 15' SRTM grids to quantify the spherical topographic mass-density anomaly effects on gravity in the study areas. Figure 3a presents the 5' × 5' grid resolution global UNB_TopoDens model while Figures 3b and 3c present the same model with higher resolution around the study areas.

4. Numerical investigations

The global spherical topographic effects on gravity at the computation points across the two test regions have first computed with constant topographic density through a global 2D numerical integration in the spatial domain to obtain reference values for further comparisons with traditional planar Bouguer correction and SRTM2gravity data. Figure 4 shows the spatial distributions of the computed values for both regions. The descriptive statistics of the data for regions N36E029 and N40E040 are presented in Tables 1 and 2, respectively, each numbered with superscript (1) in the respective table rows.

It is no surprise that the spherical gravimetric topographic effects are highly correlated with topographic variations. The spatial patterns and magnitudes are almost identical to those of the SRTM2gravity model depicted in Figure 2. The maximum values reaching up to 315 mGal in N36E029, and 385 mGal in N40E040 can be observed over the mountainous parts, while the minimums of around 18 to 30 mGal are over the seas. The standard deviations which indicate variability about the mean account for more than 70 mGal reflecting the complexity of both areas.

For the first goal of the study, the planar gravimetric terrain effects have been calculated at the computation points based on the classical approach already described in Section 2 and compared to their reference spherical counterparts displayed in Figure 4. The differences between these two datasets for each study region are illustrated in Figure 5 and statistics regarding the dataset itself, e.g., numbered with superscript (2), and the differences are given in Tables 1 and 2 for both regions, respectively. The

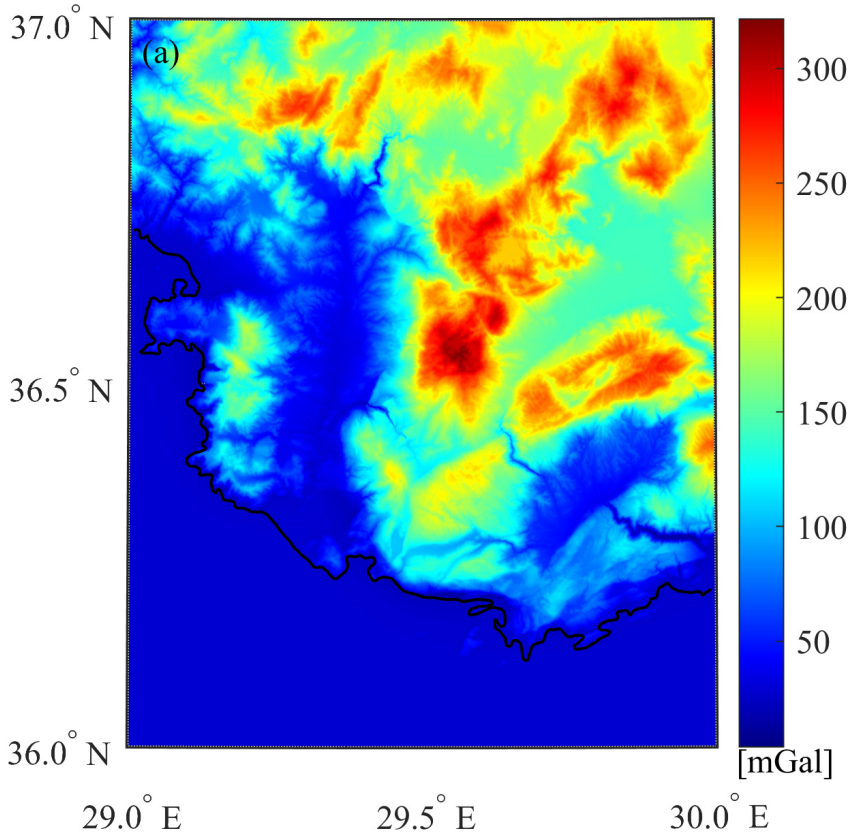
(a)
37.0° N
36.5° N
36.0° N
29.0° E
29.5° E
30.0° E
300
250
200
150
100
50
[mGal]

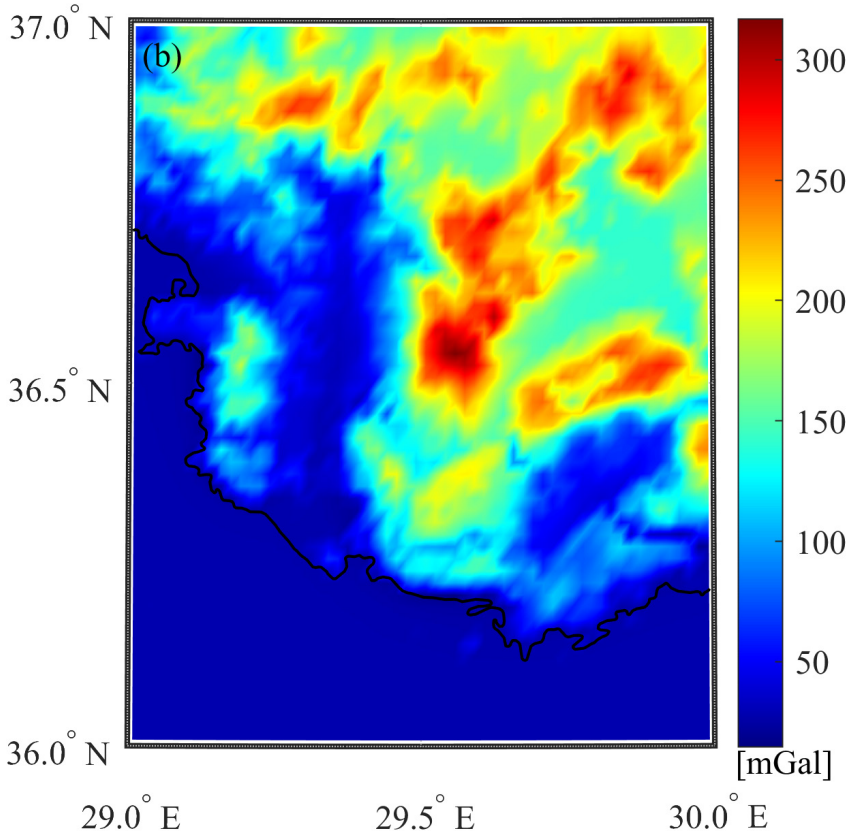
(b)
37.0° N
36.5° N
36.0° N
29.0° E
29.5° E
30.0° E
300
250
200
150
100
50
[mGal]

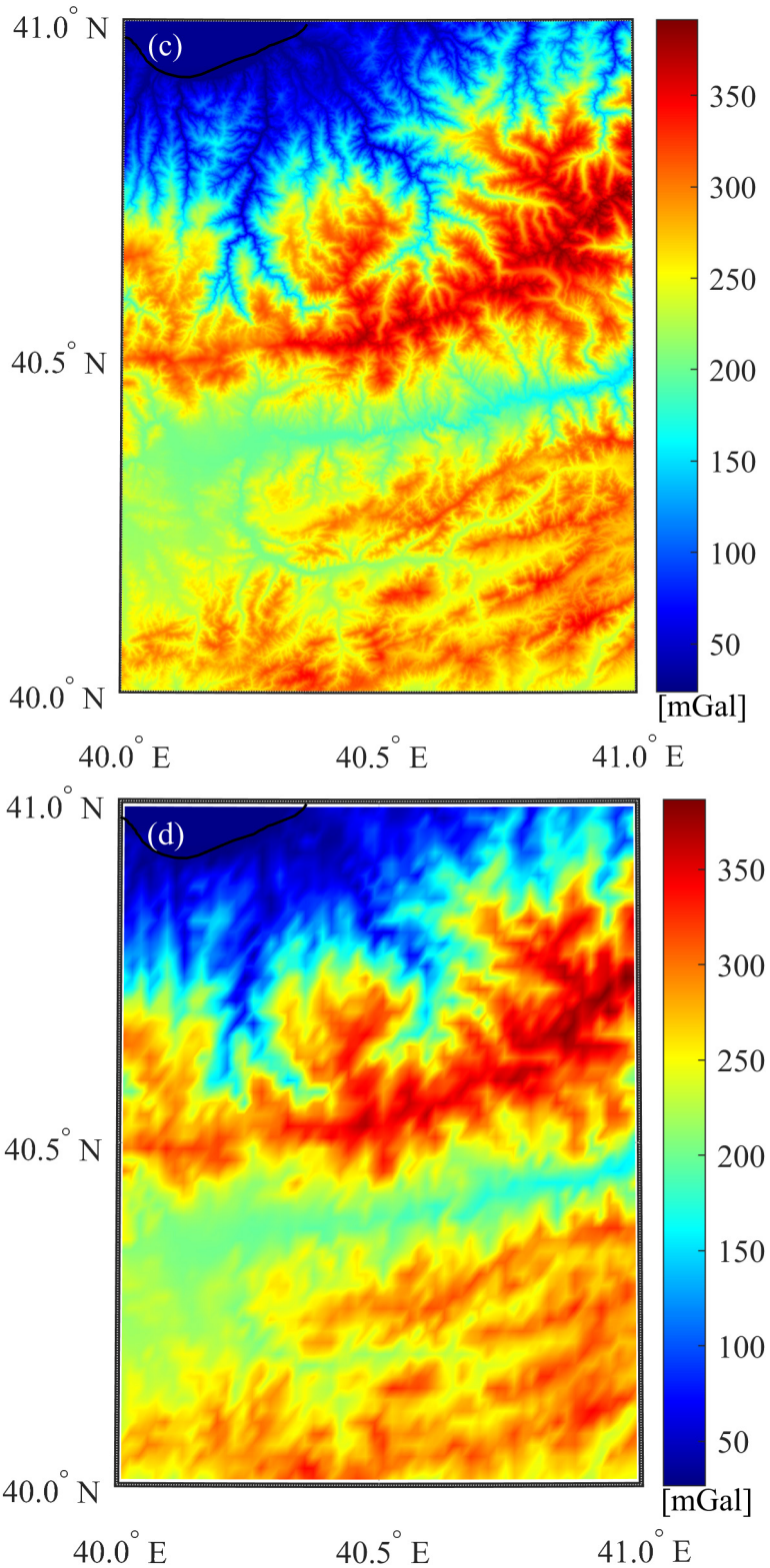

Figure 2. Ultra-high resolution SRTM2gravity spherical complete Bouguer corrections in mGal unit. (a) Original 3" × 3" grid resolution in N36E029, (b) 1' × 1' grid resolution interpolated at the computation points in N36E029, (c) Original 3" × 3" grid resolution in N40E040, (d) 1' × 1' grid resolution interpolated at the computation points in N40E040.

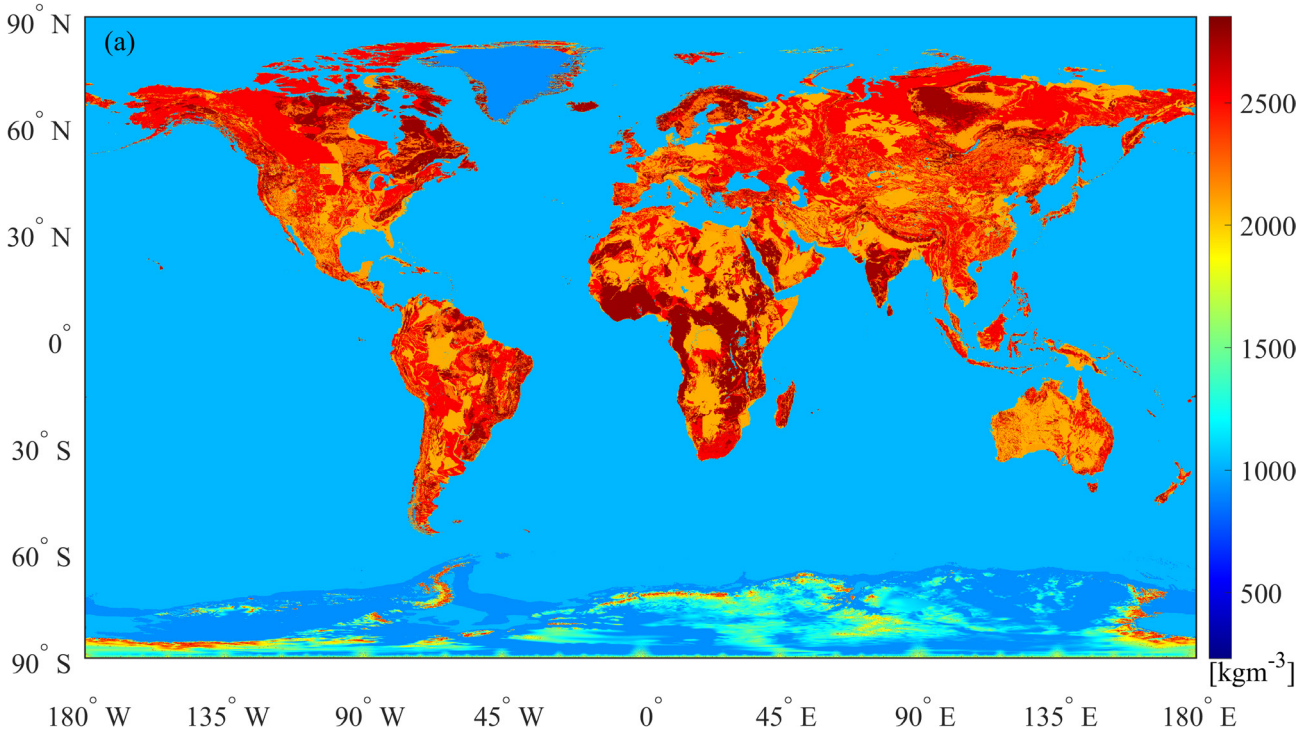
(a)
90° N
60° N
30° N
0°
30° S
60° S
90° S
180° W
135° W
90° W
45° W
0°
45° E
90° E
135° E
180° E
2500
2000
1500
1000
500
[kgm-3]

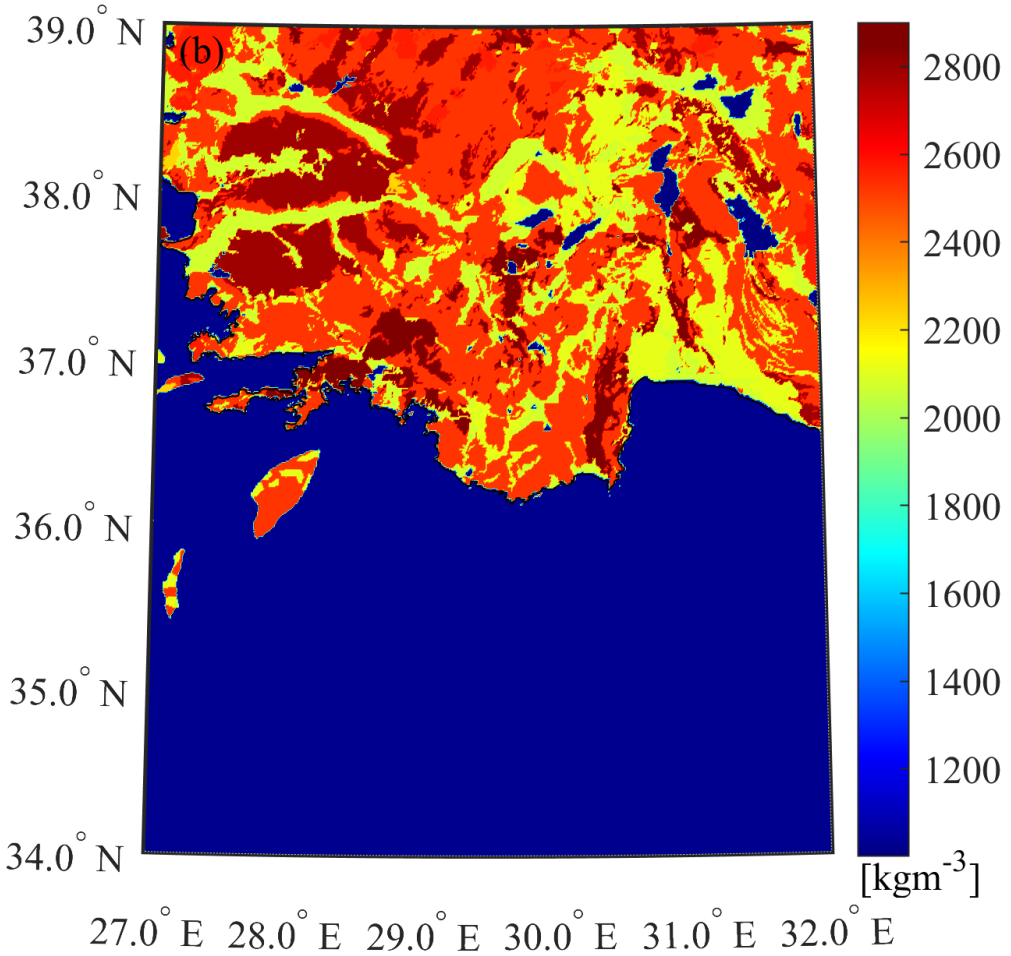
(b)
39.0° N
38.0° N
37.0° N
36.0° N
35.0° N
34.0° N
27.0° E
28.0° E
29.0° E
30.0° E
31.0° E
32.0° E
2800
2600
2400
2200
2000
1800
1600
1400
1200
[kgm-3]

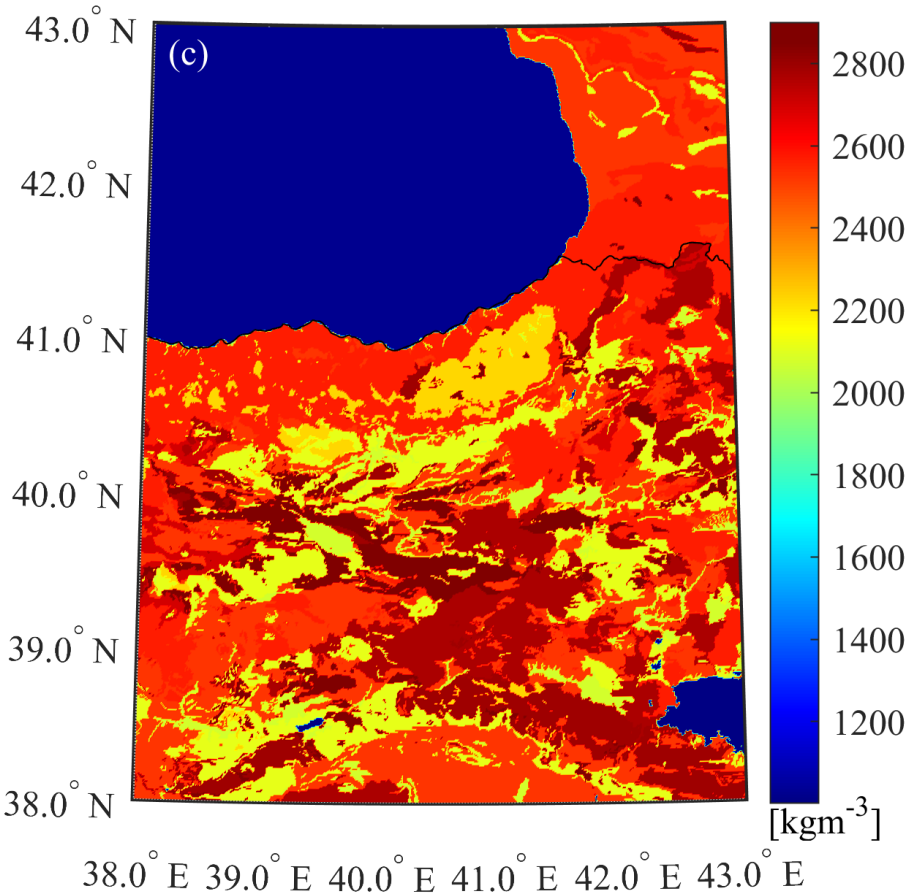

Figure 3. UNBTopoDensT_2v01 laterally varying topographical density model in kgm^{-3} unit. (a) Global distribution at 5' grid resolution, (b) Around the study area N36E029 with a higher resolution of 30", (c) Around the study area N40E040 with a higher resolution of 30".

traditional planar complete Bouguer corrections have also quite similar spatial structure to those of reference and SRTM2gravity data although not shown in the figures for brevity. While the magnitudes of each dataset change considerably, the variabilities about the means of the three datasets resemble each other strongly, i.e. around 75 mGal in N36E029 and 80 mGal in N40E040. However, the ranges between the extremes (maximums minus minimums) are again pretty close to each other. There seems an average bias of around 30 mGal between the spherical and planar gravimetric topography effects. This large difference in the mean magnitude is because the spherical Bouguer correction takes the gravitational attraction of the global topography into account while the planar one neglects the far zone effect. This is clearly illustrated in Figure 5d. The figure shows the histogram of the far zone contribution values to the planar complete Bouguer correction for both test areas. They are computed using 15' × 15' global DEM data based on point mass approximation (Wild-Pfeiffer, 2008). It is apparent that the mean of the far zone contribution is pretty close to the mean average bias between planar and spherical approaches. On the other hand, the variability of the difference between the spherical and planar Bouguer corrections is about 1 mGal which is deemed to be insignificant considering the height errors in SRTM data. These results indicate that both corrections are quite similar except for the significant difference between their means which is predominantly of a long-wavelength nature. The traditional complete planar Bouguer correction appears a good approximation of its theoretically more rigorous spherical counterparts and it does not affect the routine geophysical interpretation of the Bouguer gravity anomalies, which seeks shallow high-frequency anomalous density of masses beneath the Earth's surface. In other words, it may be useful and sufficient for gravity data inversion and interpretation in localized areas where relative values and variations rather than absolute values are sought. However, the spherical Bouguer correction is still needed especially in the geodetic boundary value problem solution and deeper-seeded anomaly exploration where

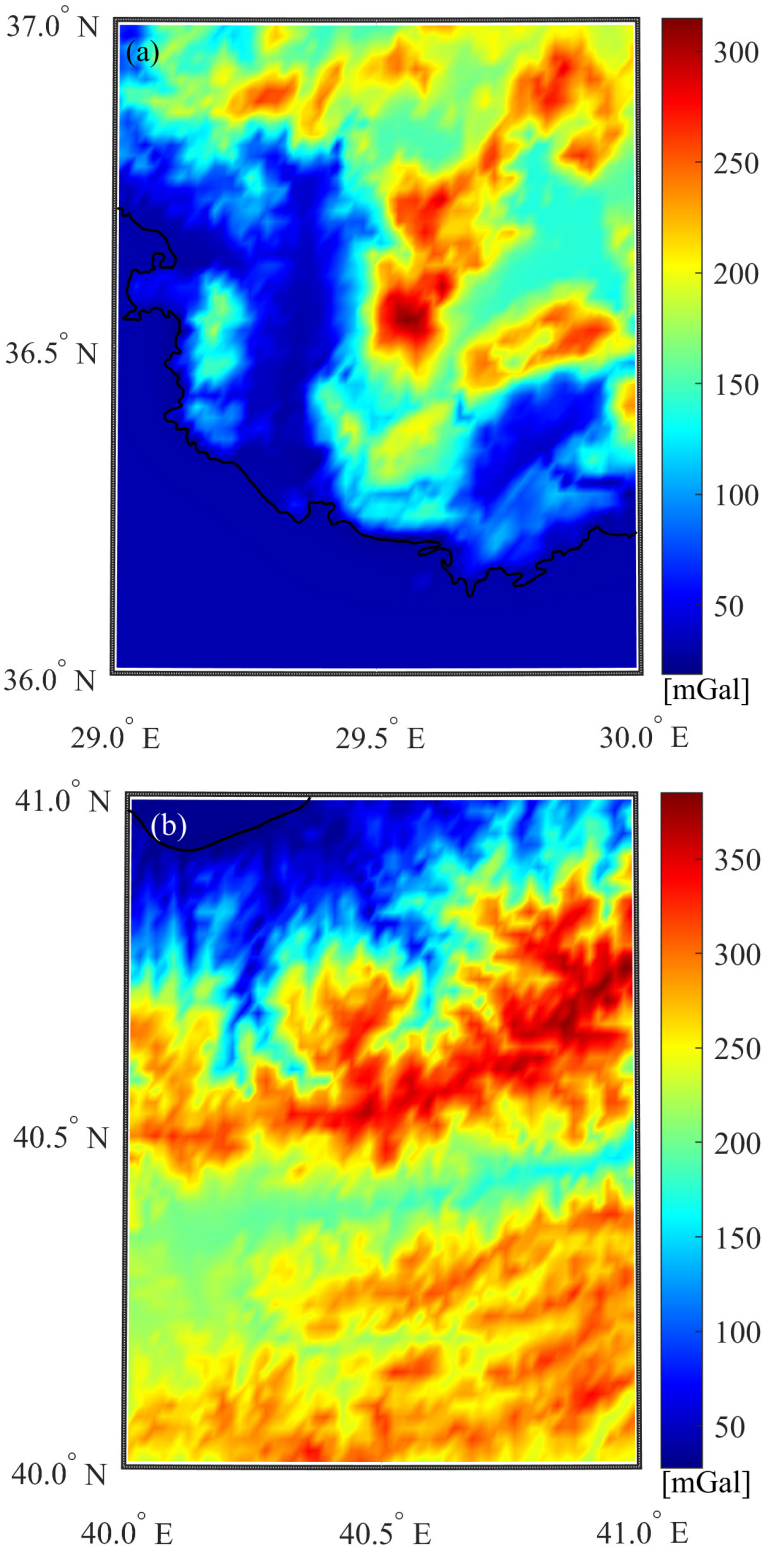

Figure 4. The reference global and spherical topographic effects computed at the 1' × 1' distributed points lying on the Earth's surface through a global 2D numerical integration in the spatial domain with 2670 kgm^{-3} constant topographic density. (a) Spatial distribution across the study area N36E029, (b) Spatial distribution across the study area N40E040.

Table 1. Some descriptive statistics of various gravimetric terrain effect data at 1' × 1' equiangular grid points on the Earth's surface distributed across the study region N36E029 (units are in mGal).

Data	Min.	Max.	Mean	Std.
(1) The reference global and spherical gravimetric topographic effects	18.62	315.04	108.10	74.46
(2) Traditional planar complete Bouguer effect	–13.08	285.27	78.88	75.05
(3) SRTM2gravity model	14.51	317.03	108.50	76.29
(4) Gravimetric effect of topo-density anomalies	–3.09	61.92	11.50	7.80
(1) minus (2)	26.85	31.84	29.21	1.65
(1) minus (3)	–4.87	9.53	–0.40	2.50

Table 2. Some descriptive statistics of various gravimetric terrain effect data at 1' × 1' equiangular grid points on the Earth's surface distributed across the study region N40E040 (units are in mGal).

Data	Min.	Max.	Mean	Std.
(1) The reference global and spherical gravimetric topographic effects	27.47	385.21	225.43	80.75
(2) Traditional planar complete Bouguer effect	–4.68	351.59	193.26	80.06
(3) SRTM2gravity model	26.60	386.85	227.41	81.13
(4) Gravimetric effect of topo-density anomalies	–1.92	61.59	27.24	15.83
(1) minus (2)	29.44	34.31	32.17	0.93
(1) minus (3)	–4.79	3.50	–1.97	0.99

not only the nearby contribution but also the far zone contribution of the global topography is required.

The SRTM2gravity model corresponding to two test areas is independently validated against the reference values from global numerical integration to achieve the second goal of the study. Figure 6 illustrates the results of the validation experiments, e.g., the difference between the two datasets, and Tables 1 and 2 present the basic statistics. The mean of the differences between SRTM2gravity values and reference values are found to be less than 2 mGal over both test areas, with the standard deviation values ranging from 0.99 mGal (N040E040) to 2.5 mGal (N36E029). Extreme differences at individual computation points never exceed a magnitude of 10 mGal over the test areas. It can easily be concluded from the figures and the statistics that the SRTM2gravity model performs considerably well in the study regions and can replace the forward global and spherical modelling of terrain effects with a constant topographic density of 2670 kgm^{-3} considering the error margins of the SRTM height data. This can effectively reduce the amount of computational cost in determining the spherical Bouguer correction for the surface observations. What is needed is to download the SRTM2gravity model freely from the provider's website and interpolate it at the observation points which is going to simplify the tedious numerical computations exceptionally.

Finally, the global 2D numerical integration in the spatial domain has been reevaluated to quantify the gravimetric effect of topo-density anomalies using the same SRTM DEMs and laterally varying density anomaly data, i.e $\Delta\rho^t(\varphi', \lambda')$ determined from UNB_TopoDens model. The contributions of topo-density anomalies to the spherical topography effects on gravity at the computation points are displayed in Figure 7 with the relevant statistics in Tables 1 and 2. Figure 7 suggests that topo-density anomalies can produce gravity anomaly effects of larger than 60 mGal, especially over the rugged topography where the density decreases noticeably below the constant value of 2670 kgm^{-3}. This can be of importance in solving the geodetic boundary value problem in which the actual density distribution of topographical masses is essential to reduce the surface observations to the geoid or mean sea level. It is also obvious from Figure 3 and Figure 7 that the near zone lateral topographic density variations have the utmost effects in producing the so-called gravity anomalies. The topo-density anomaly contribution to gravity is not distinguishable over the moderate and low-lying terrains where the lateral density variations are close to the constant density of topography and seawater.

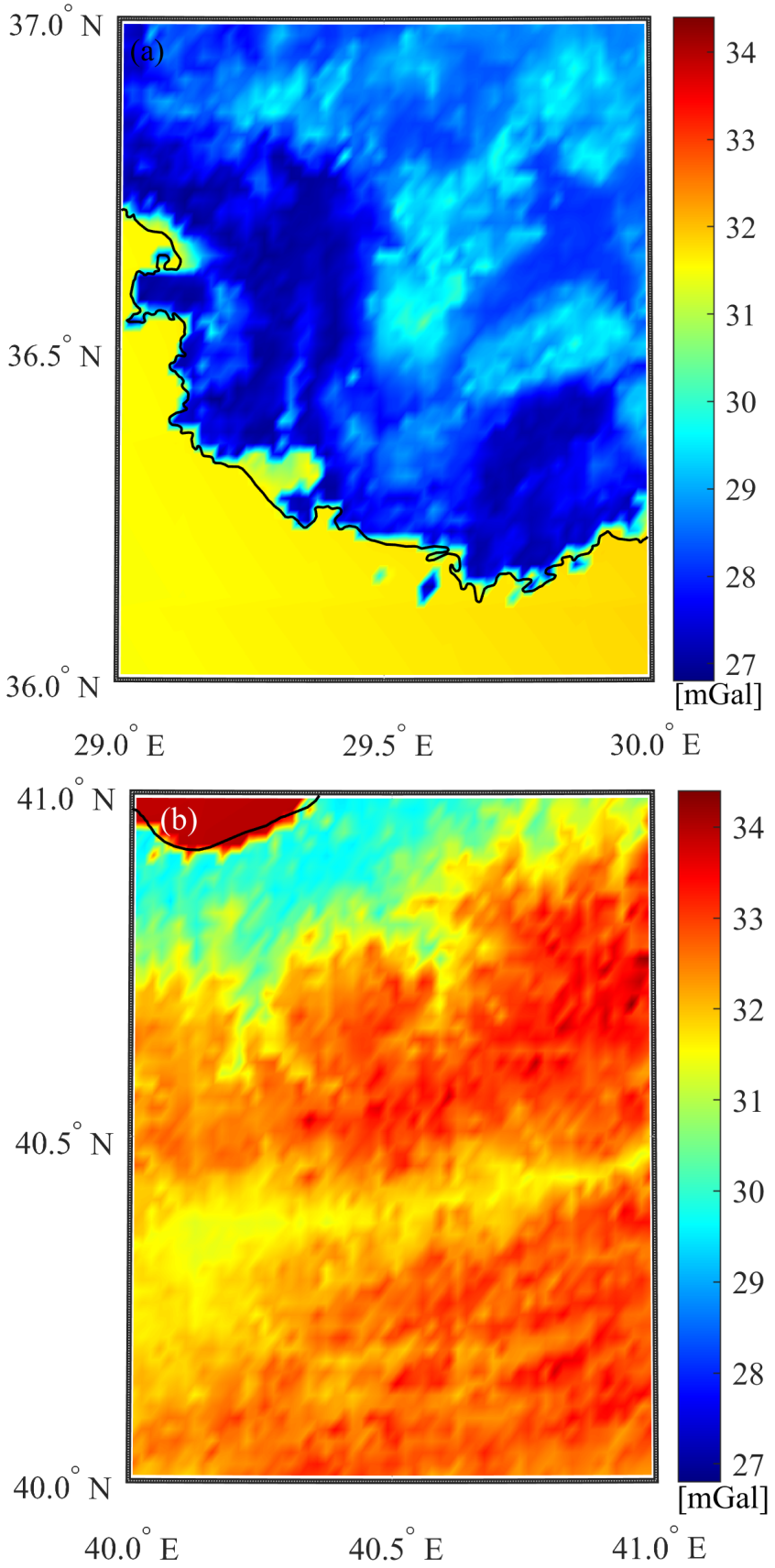
(a)
37.0° N
36.5° N
36.0° N
29.0° E
29.5° E
30.0° E
34
33
32
31
30
29
28
27
[mGal]
(b)
41.0° N
40.5° N
40.0° N
40.0° E
40.5° E
41.0° E
34
33
32
31
30
29
28
27
[mGal]

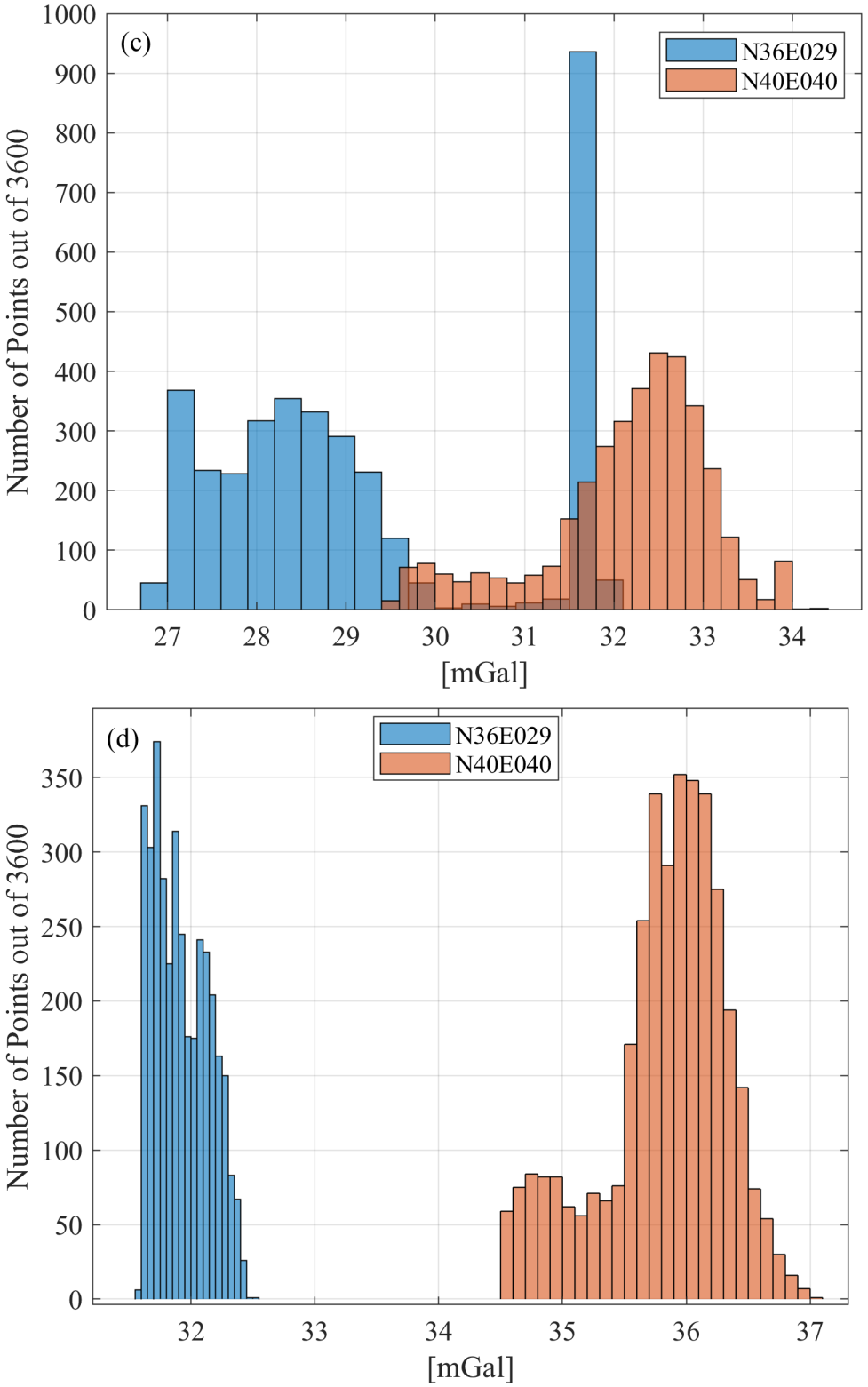

Figure 5. Differences between the reference global spherical topographic effects in Figure 4 and the traditional planar complete Bouguer effects in mGal unit. (a) Spatial distribution across the study area N36E029, (b) Spatial distribution across the study area N40E040, (c) Histogram of the differences, (d) Far zone contribution to traditional Bouguer effects.

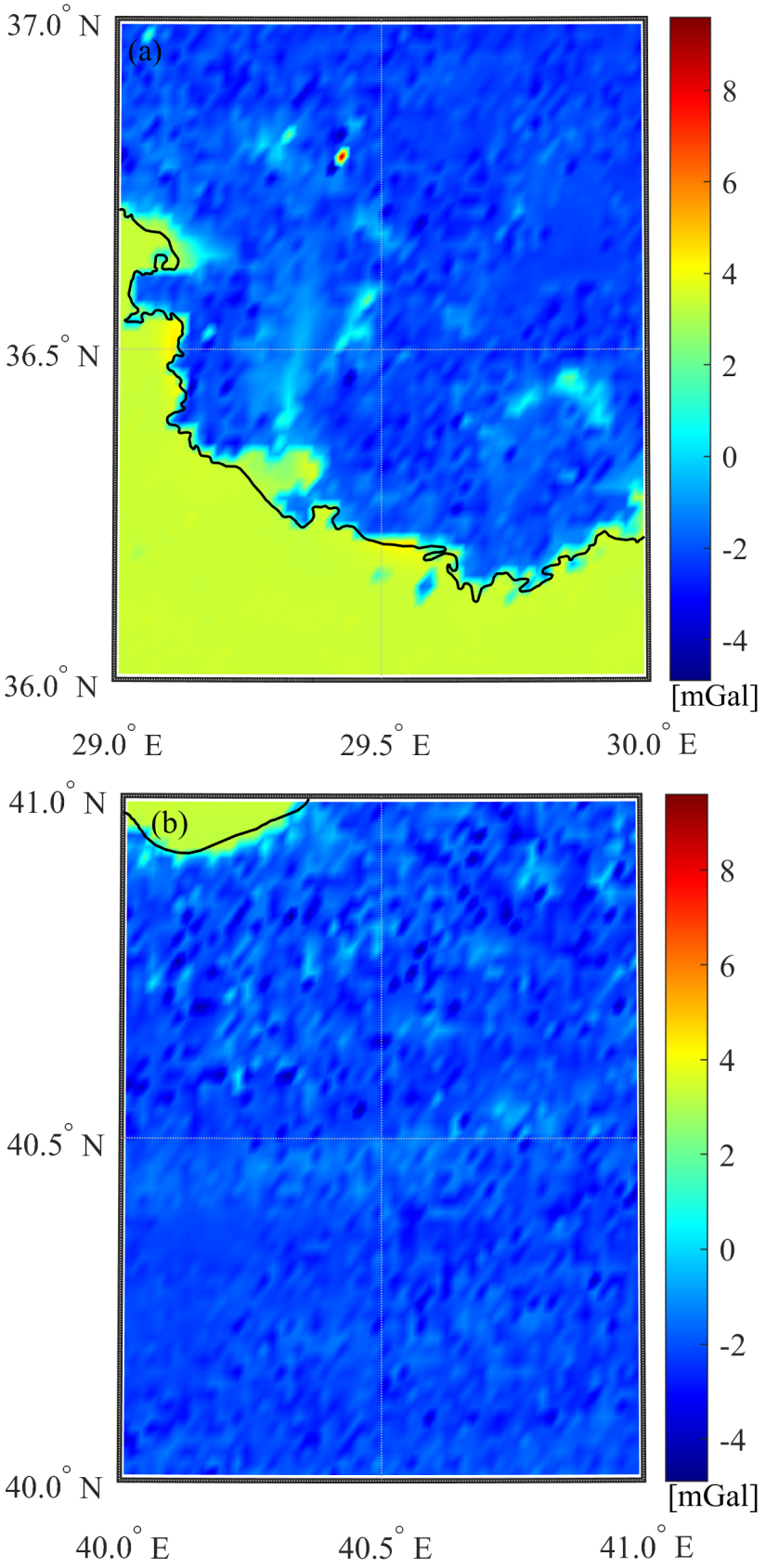
37.0° N
(a)
36.5° N
36.0° N
29.0° E
29.5° E
30.0° E
8
6
4
2
0
-2
-4
[mGal]
41.0° N
(b)
40.5° N
40.0° N
40.0° E
40.5° E
41.0° E
8
6
4
2
0
-2
-4
[mGal]

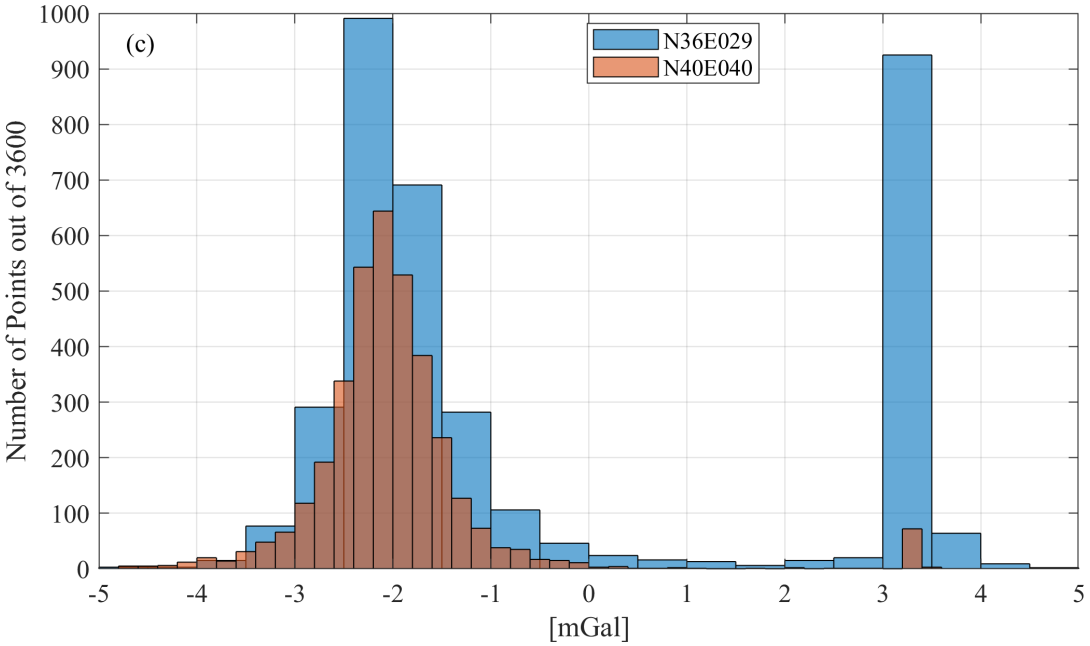

Figure 6. Differences between the reference global spherical topographic effects in Figure 4 and the SRTM2gravity model in mGal unit. (a) Spatial distribution across the study area N36E029, (b) Spatial distribution across the study area N40E040, (c) Histogram of the differences.

5. Conclusion

The spherical topographical effect on gravity computed through a global numerical integration with constant mass-density assumption has been compared to traditional planar Bouguer correction and recently released ultra-high resolution SRTM2gravity spherical Bouguer correction model at two rugged mountainous areas in Turkey. Moreover, the contribution of the anomalous topographical mass density derived from the recently released UNB_TopoDens 2D global topographical density model has been quantified in the same test regions.

The simple planar complete Bouguer corrections exhibit similar spatial characteristics to those of the spherical counterparts, but the magnitudes are different. It has been shown that the planar complete Bouguer corrections turn out to be a very good approximation in routine geophysical interpretation of the Bouguer gravity anomalies. The difference between the complete planar and complete spherical gravimetric terrain effects is around 30 mGal with a standard deviation of about 1 mGal level. This mean shift is predominantly caused by the far zone effect not accounted for in the planar approach. It can be deduced that the choice of either approach is of minor importance for most applications in the exploration of geophysics. However, the more rigorous complete spherical topography correction comprising the far zone effect is recommended for geodetic applications such as the solution of boundary value problems of potential theory to reduce the long-wavelength errors.

This study has also demonstrated that the freely available SRTM2gravity spherical complete Bouguer correction model performs exceptionally well in the test regions. The compatibility and spatial coherence between the model and reference dataset is extremely high. The spatial variations of the differences reach magnitudes of less than 10 mGal with mean and standard deviations of a few mGal levels. Considering the error margins of the SRTM2gravity model, it can be inferred from the results that the SRTM2gravity model is directly applicable to derive spherical Bouguer corrections over land areas without spending additional computational effort if one does not have previously calculated data at hand.

The solution of geodetic boundary problems requires the knowledge of global topographical density distributions to allow for a more rigorous compensation of topographical gravity effects. The topo-density anomaly-induced gravity effects can reach up to 60 mGal levels, especially over the mountainous parts of the study regions which may lead to the considerable amount of variation in terms of geoid height. It is recommended that the gravity effect of topo-density anomalies should be treated carefully and cautiously in precise geoid modelling.

The results of this study may also provide insight into the regeneration of the regional Bouguer anomaly map of Turkey. The map itself or the information derived from it finds utilization in a wide variety of applications in geosciences. It is highly recommended that the current map

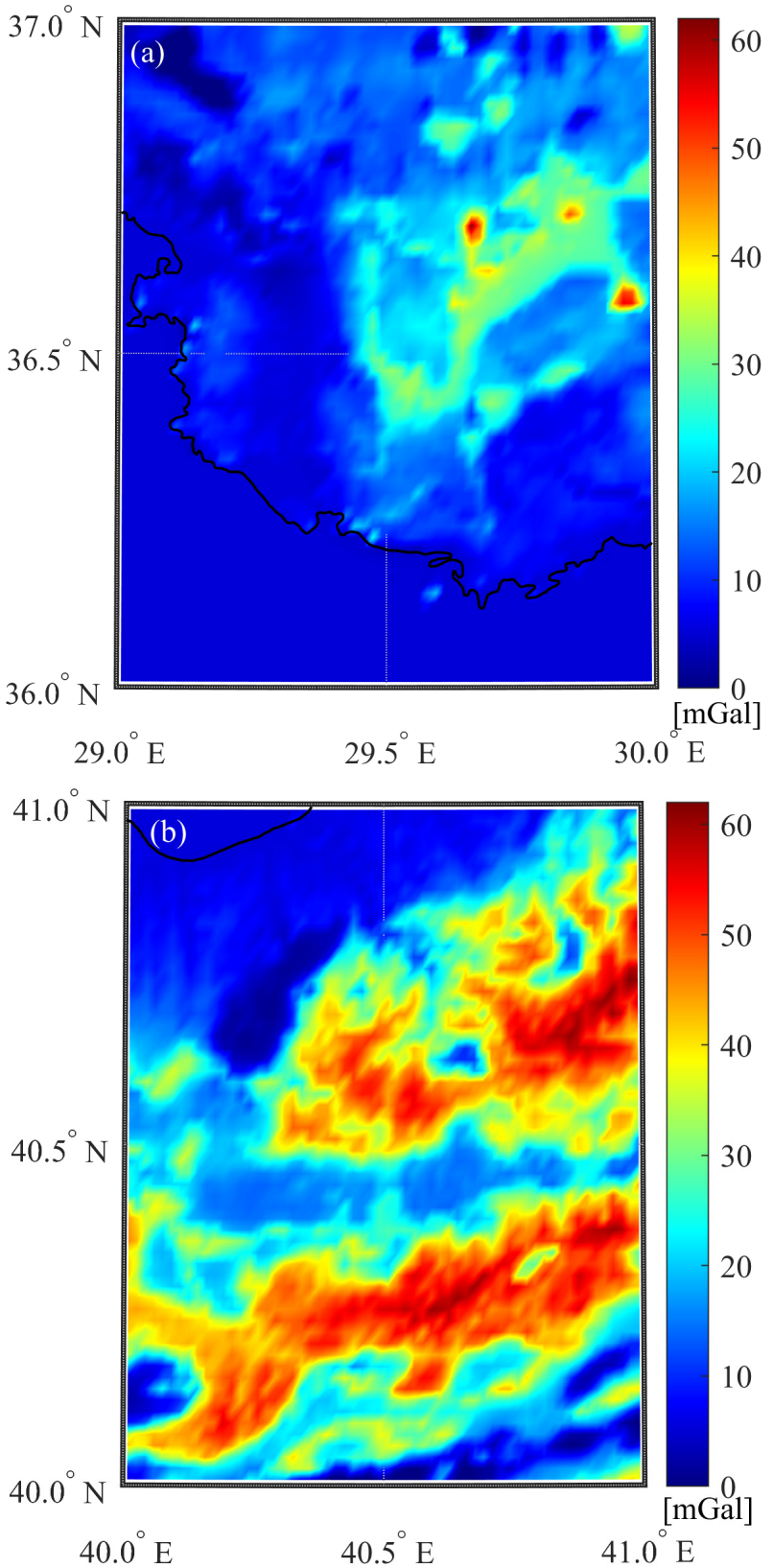

Figure 7. Gravimetric effect of topo-density anomalies in mGal unit. (a) Study area N36E029, (b) Study area N40E040.

should be modified based on contemporary techniques by replacing the traditional planar approach with global and spherical counterparts.

Acknowledgement
The author declares no conflict of interest. The MATLAB functions used in the computations can be shared upon plausible request. Please contact the corresponding author at mehmet.simav@harita.gov.tr.

References

Arslan S (2016). Geophysical regional gravity maps of Turkey and its general assessment. Bulletin of The Mineral Research and Exploration 153: 203-222. https://doi.org/10.19111/bmre.96652

Asgharzadeh MF, Von Frese RRB, Kim HR, Leftwich TE, Kim JW (2007). Spherical prism gravity effects by Gauss-Legendre quadrature integration. Geophysical Journal International 169 (1): 1-11. https://doi.org/10.1111/j.1365-246X.2007.03214.x

Becker JJ, Sandwell DT, Smith WHF, Braud J, Binder B et al. (2009). Global bathymetry and elevation data at 30 arc seconds resolution: SRTM30_PLUS. Marine Geodesy 32 (4): 355-371. https://doi.org/10.1080/01490410903297766

D'Urso MG (2013). On the evaluation of the gravity effects of polyhedral bodies and a consistent treatment of related singularities. Journal of Geodesy 87: 239-252. https://doi.org/10.1007/s00190-012-0592-1

Featherstone WE, Kirby JF (2002). New high-resolution grid of gravimetric terrain corrections over Australia. Australian Journal of Earth Sciences 49 (5): 773-774. https://doi.org/10.1046/j.1440-0952.2002.00952.x

Forsberg R (1984). A study of terrain reductions, density anomalies and geophysical inversion methods in gravity field modeling. Report No. 355, Department of Geodetic Science and Surveying, The Ohio State University, Columbus, USA. https://earthsciences.osu.edu/sites/earthsciences.osu.edu/files/report-355.pdf

Forsberg R (1985). Gravity field terrain effect computations by FFT. Bulletin Géodésique 59: 342-360. https://doi.org/10.1007/BF02521068

Grombein T, Seitz K, Heck B (2013). Optimized formulas for the gravitational field of a tesseroid. Journal of Geodesy 87: 645-660. https://doi.org/10.1007/s00190-013-0636-1

Heiskanen WA, Moritz H (1967). Physical geodesy. San Francisco, CA, USA: W.H. Freeman and Company.

Hammer S (1939). Terrain corrections for gravimeter stations. Geophysics 4 (3): 184-194. https://doi.org/10.1190/1.1440495

Heck B, Seitz K (2007). A comparison of the tesseroid, prism and point-mass approaches for mass reductions in gravity field modelling. Journal of Geodesy 81: 121-136. https://doi.org/10.1007/s00190-006-0094-0

Hinze WJ, von Frese RRB, Saad AH (2013). Gravity and Magnetic Exploration: Principles, Practices and Applications. New York: Cambridge University Press. https://doi.org/10.1017/CBO9780511843129

Hirt C, Yang M, Kuhn M, Bucha B, Kurzmann A et al. (2019). SRTM2gravity: An ultrahigh resolution global model of gravimetric terrain corrections. Geophysical Research Letters 46 (9): 4618-4627. https://doi.org/10.1029/2019GL082521

Kuhn M, Featherstone WE, Kirby JF (2009). Complete spherical Bouguer gravity anomalies over Australia. Australian Journal of Earth Sciences 56 (2): 213-223. https://doi.org/10.1080/08120090802547041

Li YC, Sideris MG (1994). Improved gravimetric terrain corrections. Geophysical Journal International, 119 (3): 740-752. https://doi.org/10.1111/j.1365-246X.1994.tb04013.x

Martinec Z, Vaníček P, Mainville A, Véronneau M (1996). Evaluation of topographical effects in precise geoid computation from densely sampled heights. Journal of Geodesy 70: 746-754. https://doi.org/10.1007/BF00867153

Martinec Z (1998). Boundary value problems for gravimetric determination of a precise geoid. Lecture notes in Earth Sciences 73. Springer, Berlin Heidelberg New York.

McCubbine JC, Featherstone WE, Kirby JF (2017). Fast-Fourier-based error propagation for the gravimetric terrain correction. Geophysics 82 (4): 71-76. https://doi.org/10.1190/geo2016-0627.1

Moritz H (1968). On the use of the terrain correction in solving Molodensky's problem. Report No. 108, Department of Geodetic Science, The Ohio State University, Columbus

Nagy D (1966). The gravitational attraction of a right rectangular prism. Geophysics 31 (2): 362–371. https://doi.org/10.1190/1.1439779

Nagy D, Papp G, Benedek J (2000). The gravitational potential and its derivatives for the prism. Journal of Geodesy 74: 552-560. https://doi.org/10.1007/s001900000116

Novák P (2000). Evaluation of gravity data for the Stokes-Helmert solution to the geodetic boundary-value problem. Technical Report No. 207, UNB, Fredericton, Canada.

Novák P, Vaníček P, Martinec Z, Véronneau M (2001) Effects of the spherical terrain on gravity and the geoid. Journal of Geodesy 75: 491–504. https://doi.org/10.1007/s001900100201

Olson CJ, Becker JJ, Sandwell DT (2016). SRTM15_PLUS: Data fusion of Shuttle Radar Topography Mission (SRTM) land topography with measured and estimated seafloor topography. NCEI Accession 0150537.

Sheng MB, Vaníček P, Kingdon RW, Santos M, Foroughi I (2019). Formulation and validation of a global laterally varying topographical density model. Tectonophysics 762: 45-60. https://doi.org/10.1016/j.tecto.2019.04.005

Sideris MG (1985). A fast Fourier transform method for computing terrain corrections. Manuscripta Geodaetica 10: 66–73.

Simav M, Yıldız H (2021). Quantifying the bathymetric stripping gravity corrections of global seawater and major lakes over Turkey. Turkish Journal of Earth Sciences 30: 916-927. https://doi.org/10.3906/yer-2105-38.

Tozer B, Sandwell DT, Smith WHF, Olson C, Beale JR et al. (2019). Global bathymetry and topography at 15 arcsec: SRTM15+. Earth and Space Science 6 (10): 1847-1864. https://doi.org/10.1029/2019EA000658

Tsoulis D (2001). Terrain correction computations for a densely sampled DTM in the Bavarian Alps. Journal of Geodesy 75: 291-307. https://doi.org/10.1007/s001900100176

Tsoulis D (2012). Analytical computation of the full gravity tensor of a homogeneous arbitrarily shaped polyhedral source using line integrals. Geophysics 77 (2): F1–F11. https://doi.org/10.1190/geo2010-0334.1

Uieda L, Barbosa VCF, Braitenberg C (2016). Tesseroids: Forward-modeling gravitational fields in spherical coordinates. Geophysics 81 (4): F41-F48. https://doi.org/10.1190/geo2015-0204.1

Vajda P, Vaníček P, Novák P, Meurers B (2004). On evaluation of Newton integrals in geodetic coordinates: Exact formulation and spherical approximation. Contributions to Geophysics and Geodesy 34 (4): 289-314.

Vajda P, Foroughi I, Vaníček P, Kingdon R, Santos M et al. (2020). Topographic gravimetric effects in earth sciences: Review of origin, significance and implications. Earth-Science Reviews 211: 103428. https://doi.org/10.1016/j.earscirev.2020.103428

Wessel P, Luis JF, Uieda L, Scharroo R, Wobbe F et al. (2019). The Generic Mapping Tools version 6. Geochemistry, Geophysics, Geosystems 20 (11): 5556-5564. https://doi.org/10.1029/2019GC008515

Wild-Pfeiffer F (2008). A comparison of different mass elements for use in gravity gradiometry. Journal of Geodesy 82: 637-653. https://doi.org/10.1007/s00190-008-0219-8

Yamazaki D, Ikeshima D, Tawatari R, Yamaguchi T, O'Loughlin F et al. (2017). A high accuracy map of global terrain elevations. Geophysical Research Letters 44 (11): 5844-5853. https://doi.org/10.1002/2017GL072874

Yang M, Hirt C, Pail R (2020). TGF: A new MATLAB-based software for terrain-related gravity field calculations. Remote Sensing 12 (7): 1063. https://doi.org/10.3390/rs12071063